

ARTICLE

Received 1 Jun 2011 | Accepted 28 Oct 2011 | Published 29 Nov 2011

DOI: 10.1038/ncomms1578

# Sauropod dinosaur osteoderms from the Late Cretaceous of Madagascar

Kristina Curry Rogers<sup>1</sup>, Michael D'Emic<sup>2</sup>, Raymond Rogers<sup>1</sup>, Matthew Vickaryous<sup>3</sup> & Amanda Cagan<sup>1</sup>

Osteoderms are bones embedded within the dermis, and are common to select members of most major tetrapod lineages. The largest known animals that bear osteoderms are members of Titanosauria, a diverse clade of sauropod dinosaurs. Here we report on two titanosaur osteoderms recovered from the Upper Cretaceous Maevarano Formation of Madagascar. Each osteoderm was discovered in association with a partial skeleton representing a distinct ontogenetic stage of the titanosaur *Rapetosaurus krausei*. Combined, these specimens provide novel insights into the arrangement and function of titanosaur osteoderms. Taphonomic data confirm that *Rapetosaurus* developed only limited numbers of osteoderms in its integument. The adult-sized osteoderm is the most massive integumentary skeletal element yet discovered, with an estimated volume of 9.63 litres. Uniquely, this specimen possesses an internal cavity equivalent to more than half its total volume. Large, hollow osteoderms may have functioned as mineral stores in fecund, rapidly growing titanosaurs inhabiting stressed environments.

<sup>1</sup> Biology and Geology Departments, Macalester College, 1600 Grand Avenue, St. Paul, Minnesota 55105, USA, <sup>2</sup> Geology and Geography Department, Georgia Southern University, Box 8149, Statesboro, GA 30460, USA. <sup>3</sup> Ontario Veterinary College, University of Guelph, 50 Stone Road, Guelph, ON, Canada. Correspondence and requests for materials should be addressed to K.C.R. (email: rogersk@macalester.edu).

Osteoderms are widely distributed among archosaurs including crocodylomorphs, aetosaurs and dinosaurs<sup>1–6</sup>. Among dinosaurs, osteoderms are best known from the ornithischian clades Ankylosauria<sup>7</sup> and Stegosauria<sup>8,9</sup>, where they develop into a variety of plate- and spine-shaped elements and have a characteristic paramedian distribution as multiple rows enveloping the dorsolateral body surface. Among saurischians, osteoderms have been reported for a single carnivorous dinosaur, the ceratosaurian *Ceratosaurus*<sup>10</sup>, and a number of titanosaurian sauropods<sup>4–6</sup>.

Titanosauria is a diverse clade of sauropods that attained a global distribution by the end of the Cretaceous Period, and includes both the largest terrestrial vertebrates yet known and small-bodied dwarfs<sup>6</sup>. Titanosaurs are the only sauropods known to possess osteoderms, although specific details of the taxonomic identity, anatomical distribution, evolution, and potential function(s) of these elements remain a mystery<sup>4</sup>.

Here we report on two recently recovered osteoderms that represent different stages of skeletal ontogeny (Fig. 1). Significantly, these elements reveal that the enormous size of at least some adult *Rapetosaurus* osteoderms is accompanied by the presence of a large, hollow cavity (Figs 1h, 2).

## Results

**Location.** The new osteoderms were recovered from locality MAD 93-18 in the Anembalemba Member of the Maevarano Formation (Maastrichtian)<sup>11</sup>. MAD 93-18 includes at least three bone-bearing horizons that yield well-preserved skeletal remains of *Rapetosaurus*<sup>6,12</sup>.

**Juvenile *Rapetosaurus* osteoderm anatomy.** UA (Université d'Antananarivo) 9331, the smallest osteoderm, was collected in association

with the caudal vertebrae of a partially articulated skeleton of a juvenile *Rapetosaurus* (femur length = ~75 cm) in the uppermost bonebed of MAD 93-18. UA 9331 is an ellipsoid osteoderm that measures 14.4 cm × 9.2 cm × 6.9 cm. Except for a low-relief, relatively smooth midpoint convexity, the majority of the external bone texture of UA 9331 is rugose, characterized by thin, disorganized and densely packed mineralized fibres (Fig. 1c–e). Computed tomographic (CT) scans demonstrate that the pristinely preserved outer cortex of dense, compact bone is underlain by a cancellous core of bony trabeculae similar to that of other amniote osteoderms<sup>1–4</sup> (Fig. 1e). Of particular note is a prominent canal that passes uninterrupted through the element (Fig. 1c–e). As evidenced by CT scans, this canal widens to form a cavity midway into the osteoderm, within the otherwise cancellous core of the element (Fig. 1e). A distinct radiopaque layer of compact bone lines this cavity. CT scans also reveal a horizon of radiopaque compact bone deep within the cancellous core that spans the long axis of the element and intersects with the cavity (Fig. 1e).

**Adult *Rapetosaurus* osteoderm anatomy.** FMNH PR (Field Museum of Natural History) 2342, the large osteoderm, was recovered in close association with right and left ischia of an adult-sized *Rapetosaurus* skeleton (femur length = 146 cm) in the basal bonebed of MAD 93-18. This osteoderm measures 57.2 cm × 26.7 cm × 19.2 cm in maximum dimensions and has an estimated volume of 9.63 l, making it the most massive osteoderm ever discovered (Figs 1a,b,f–h and 2). Overall, it resembles an ellipsoid and exhibits the bulb and root morphology noted for some other titanosaur osteoderms<sup>4</sup>. A large ovoid depression on the external surface of the osteoderm reflects damage to the relatively smooth, flat, circular

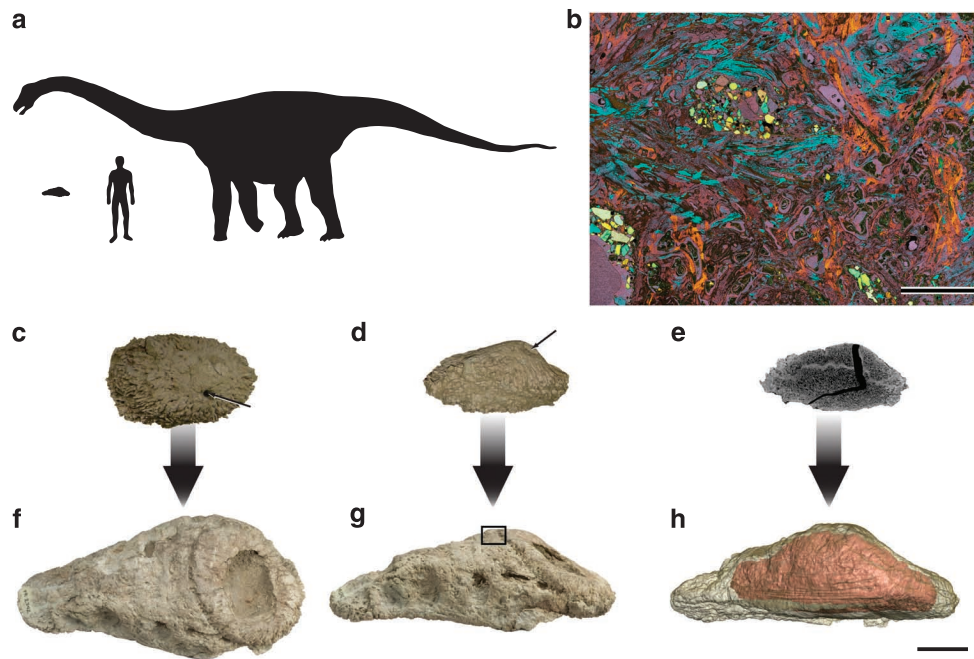


**Figure 1 | *Rapetosaurus krausei* osteoderm morphology at two different ontogenetic stages.** (a) Silhouette drawings of an adult *Rapetosaurus krausei* osteoderm (FMNH PR 2342), a 1.8-m-tall human, and an adult specimen of *Rapetosaurus krausei*, highlighting the large size of the osteoderm. (b) Bone histology of the adult osteoderm of *Rapetosaurus krausei*, showing densely remodelled, intersecting spicules of fibrolamellar bone and internal resorption cavities and 0.5 cm scale bar. Location of thin section is indicated by the box in g. (c–e) Osteoderm pertaining to a juvenile specimen of *Rapetosaurus krausei* (UA 9331) with 5 cm scale bar in c, external; d, lateral, e, CT-generated slice illustrating the highly vascularized internal anatomy of this osteoderm. A 2D projection of the twisting sinus that passes through the osteoderm is shown in black. Arrows in c and d indicate one exit of this sinus. (f–h) Adult osteoderm of *Rapetosaurus krausei* with 10 cm scale bar in f, external view, depression at right is result of damage during excavation and is not a primary anatomical characteristic. (g) Lateral view with box showing location of histological section shown in b, and h, isometric CT reconstruction with exterior bone rendered transparent and internal cavity (volume = 4.88 litres) shown in pink. Wide arrows between c–e and f, g indicate the possible ontogenetic development of *Rapetosaurus* osteoderms. The total volume of the adult osteoderm is 9.63 l.

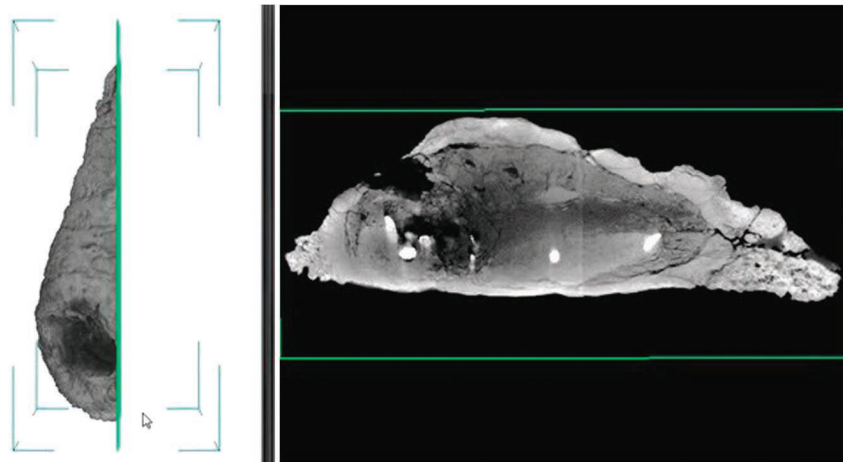


**Figure 2 | CT-scan image of an adult *Rapetosaurus krausei* osteoderm.** The CT scan shows the internal void in FMNH PR 2342, an adult *Rapetosaurus krausei* osteoderm. The void is filled with unconsolidated sediment. Radio-opaque internal bright spots are secondary deposits of barite (common in Maevarano Formation fossils). The cavity is ~4.9 litres in volume, with the thickness of bone surrounding the external cavity ranging from 1.2 to 3.5 cm.

bulb during collection, and is not a primary anatomical characteristic (Fig. 1f). The deep surface is characterized by an orthogonal or cross-hatched texture of mineralized fibres punctuated by numerous foramina, whereas the superficial surfaces are relatively smooth and more sparsely vascularized. CT scans (Fig. 1h) and exploratory cores (Fig. 1b) taken for histological purposes reveal that FMNH PR 2342 is hollow. The void is filled with unconsolidated sediment and contains no broken internal trabeculae. This cavity is ~4.9 l in volume, representing more than 50% of the total volume of the osteoderm. The thickness of bone surrounding this inner cavity varies from 1.2 to 3.5 cm (Fig. 1f,h). The inner bony margin of the cavity shows resorptive lacunae consistent with osteoclastic resorption<sup>13–15</sup> and grades into heavily remodelled fibrolamellar bone (Fig. 1b).

## Discussion

These two specimens represent examples of both juvenile and adult *Rapetosaurus* osteoderm development. The structural organization (compact cortex, cancellous core) and bone histology of the juvenile specimen (UA 9331) are broadly comparable with those of other archosaurs<sup>1–4,7</sup>. In contrast, the gross anatomical and microscopic structure of the adult-sized specimen (FMNH PR 2342) is unique. The shape and surface texture of *Rapetosaurus* osteoderms indicates that these elements were low in relief and embedded in the integument as in other vertebrates<sup>1–3,14,16</sup>. As evidenced from extant taxa, all osteoderms form and reside within the dermis, either adjacent to the interface between the *strata superficiale* and *compactum*, or exclusively within the *stratum superficiale*, and are overlain by the epidermis<sup>1–3,14–17</sup>. The surface texture of *Rapetosaurus* osteoderms is consistent with the hypothesis that, as in crown group archosaurs, these structures were overlain by epidermal scales<sup>1–3</sup>. The hollow nature of the adult specimen is unique, and we speculate that the juvenile morph remodels to achieve the adult form. We propose that the initially modest vascular sinus present in the juvenile specimen could represent the locus for calcium remobilization and remodelling, resulting in a well-defined hollow rimmed by heavily remodelled bone tissue at the adult stage (Fig. 1).

Although osteoderms are a commonly cited feature of titanosaurs, they are relatively rare, with only about 90 specimens known worldwide<sup>4</sup>. Thus, it is not surprising that only 10 osteoderms have been collected among the 141 titanosaur-bearing localities in the Maevarano Formation<sup>5,6,12,18</sup>. Sedimentologic data indicate that recurrent fine-grained debris flows were the predominant burial

mechanism for Maevarano Formation vertebrates<sup>11,19,20</sup>. These viscous debris flows would not have readily entrained and winnowed osteoderms from their respective skeletons, but are predicted to bury them in close proximity to other skeletal remains, as is the case with crocodylomorphs recovered from the same formation<sup>19</sup>. Accordingly, we reason that the integument of *Rapetosaurus* was not heavily invested with osteoderms. Instead, we hypothesize that *Rapetosaurus* (and probably most titanosaurs) was characterized by a small number of osteoderms. Furthermore, unlike many osteoderm-bearing archosaurs<sup>1–3</sup>, these elements did not develop pervasively throughout the dermis but were probably restricted to the isolated regions of the integument. Whereas previous descriptions had reported the presence of articulating mosaics of osteoderms from the Maevarano formation<sup>5</sup>, we reinterpret these ‘mosaics’ as the fragmentary remains of individual adult-sized cavities that were crushed post-mortem. To date, at least four Maevarano Formation osteoderm occurrences consist of these fragmentary remnants of large adult specimens.

Although titanosaur phylogeny is currently labile, all published cladograms require multiple independent gains and/or losses of osteoderms<sup>4,6,21</sup>. This pattern may be genuine, as osteoderms have a sporadic phylogenetic distribution in other clades, with independent evolution of osteoderms at least eight times within Amniota, and at least four times within Archosauria<sup>1–3</sup>. However, in light of the fragile nature of hollow titanosaur osteoderms, some of the perceived losses of osteoderms in titanosaur evolution are more likely attributable to taphonomy. With regard to potential function, osteoderms are often assumed to have a protective role, but this is unlikely for *Rapetosaurus* osteoderms, because they do not form the imbricated ‘armour’ observed in other vertebrates<sup>1–3,16,22–24</sup>. Moreover, protective benefits would seemingly decrease in the vacuous, thin-walled adult structures. Thermoregulatory functions, proposed for osteoderms in crocodylomorphs<sup>1–3,22</sup> and squamates<sup>1,25,26</sup>, are unlikely for *Rapetosaurus* because its osteoderms are arguably too rare to be effective, especially with their low surface area–volume ratios. The lack of an osteoderm ‘pavement’ or ‘shield’ also precludes biomechanical support during locomotion as proposed for crocodyli-forms<sup>27</sup>. Display, including mate and species recognition, is probably the most commonly cited explanation for dinosaur osteoderms<sup>7–10</sup>, but *Rapetosaurus* osteoderms are nondescript in comparison to the elaborate bony display structures of other dinosaurs<sup>7,10</sup>, especially when considered in the context of adult body size<sup>4,6,12</sup>. Moreover, similarly shaped ellipsoid osteoderms have been attributed to five

other titanosaurs on as many continents<sup>4</sup>, reducing the likelihood of a widespread role in species individuation<sup>7,9</sup>. Finally, the discovery of several other hollow osteoderms in the Maevarano formation precludes both pathology and individual variation as causes of the internal cavity observed in adult *Rapetosaurus*.

Given the above considerations, we are reluctant to attribute any of the aforementioned functions to the unusual *Rapetosaurus* osteoderms. Instead, we propose that they might have served as a mineral reservoir. Osteoclastic remodelling of bone mineral is necessary for blood calcium homeostasis<sup>15,27–29</sup> and increases seasonally<sup>30</sup>, during oogenesis<sup>23</sup>, and with increased age<sup>13</sup> in extant animals. Osteoderms are often associated with complex vascular networks, including numerous small diameter anastomosing arteries and veins within the *stratum superficiale*<sup>3,14,16,22,25,26,31,32</sup>. These vessels then join larger diameter subcutaneous arterioles and venules<sup>22,25,26,32</sup>. These vascular networks facilitate thermoregulation in some crocodylians<sup>22</sup> and lizards<sup>25</sup>, and also serve as conduits for mobilized mineral reserves from the integument<sup>23,25,26,30</sup>. Like most other sauropods, titanosaurs like *Rapetosaurus* rapidly attained skeletal maturity<sup>32</sup> and exhibited comparatively high levels of fecundity<sup>33</sup>, both of which place demands on bone mineral reserves<sup>13,15,22,23,28,29,34,35</sup>. Moreover, *Rapetosaurus* inhabited a highly seasonal, semi-arid setting that was characterized by periodic, intense droughts that resulted in recurrent mass mortality<sup>19,20</sup>. Only six of the ten other known osteoderm-bearing titanosaurs are derived from well-documented palaeoenvironmental contexts<sup>4</sup>. These taxa also inhabited seasonal, semi-arid to arid palaeoenvironments<sup>36–41</sup>.

Under these palaeoenvironmental conditions, we propose that osteoderms may have provided an important, adaptive, integumentary mineral reservoir throughout *Rapetosaurus* life history (and perhaps in other osteoderm-bearing titanosaurs). In response to physiological demands, calcium and phosphorous were presumably redeployed through osteoclasia and mobilized within a dermal vascular network resulting in the formation of large interior cavities. Under prolonged and/or recurrent stress, it is possible that osteoderms were so extensively remodelled that they became either unrecognizable as distinct elements or too fragile to survive the rigours of burial and fossilization, both of which would account for their rarity in the Maevarano Formation, and the titanosaur record in general.

Adult *Rapetosaurus* bore a few massive, but internally hollow, integumentary skeletal elements. The internal hollow appears to develop through remodelling of the cancellous core observed at juvenile ontogenetic stages, and may have functional implications for mineral storage in fecund, rapidly growing titanosaurs inhabiting stressed environments.

## Methods

**Computed tomography.** CT scanning of FMNH 2342 was done on an NSI M5000 digital real-time and computed tomography system provided by North Star Imaging. A 'Cone-Beam' CT scan was performed acquiring 720 two-dimensional (2D) images during a 360° rotation of the specimen-yielding images at 0.5 degree increments. Resolution of the detector was 2,048×2,048 pixels with magnification of ×1.25 providing an optimum effective three-dimensional (3D) voxel resolution of ~155 microns. The sample was scanned in two halves with maximum penetration power of 450 kV. The smaller specimen was scanned on an NSI M5000 digital real-time system with an effective 3D voxel resolution of ~75 microns. The volume of the interior void of FMNH PR 2342 was calculated with software provided by Kinetic Vision via a technique called segmentation, in which pixels are selected either automatically, semi-automatically, or manually on a set of successive 2D images. These 2D images make up a 3D volume when stacked together. Automatic/semi-automatic selection of pixels is based on the iso-value correlating to each pixel of the data set. Once automatic segmentation is complete manual segmentation allowed clean up of areas where noise occurs. The selected pixels are then designated to a material label (for example, exterior surface or interior void). Once the pixels of interest are correctly assigned to a material, then the volume of each material was calculated: FMNH PR 2342 total volume = 9,627,075.5 mm<sup>3</sup>; FMNH PR 2342 interior void volume = 4,880,507.5 mm<sup>3</sup> (Fig. 2, Supplementary Movie 1).

**Histological analysis.** Two areas of FMNH PR 2342 were cored with a diamond-coated drill bit perpendicular to the long axis of the element for histological analysis. The first core came from the intersection of the bulb and root (Fig. 1). A second core came from the external surface of the root. Cores were embedded in epoxy resin and mounted to glass slides. Thin-sections were made with an Isomet slow speed diamond saw and hand ground on a lapidary wheel until ~60–80 μm thick. Observations/measurements were made with regular and cross-polarized microscope. Copies of thin-sections are located at Macalester College and in the Field Museum of Natural History.

## References

- Vickaryous, M. K. & Sire, J.-Y. The integumentary skeleton of tetrapods: origin, evolution, and development. *J. Anat.* **214**, 441–464 (2009).
- Hill, R. V. Integrative morphological data sets for phylogenetic analysis of Amniota: the importance of integumentary characters and increased taxonomic sampling. *Syst. Biol.* **54**, 530–547 (2005).
- Vickaryous, M. K. & Hall, B. K. Development of the dermal skeleton in *Alligator mississippiensis* (Archosauria, Crocodylia) with comments on the homology of osteoderms. *J. Morphol.* **269**, 398–422 (2008).
- D'Emic, M. D., Wilson, J. A. & Chatterjee, S. The titanosaur (Dinosauria: Sauropoda) osteoderm record: review and first definitive specimen from India. *J. Vertebr. Paleontol.* **29**, 165–177 (2009).
- Dodson, P., Krause, D. W., Forster, C. A., Sampson, S. D. & Ravoavy, F. Titanosaurid (Sauropoda) osteoderms from the Late Cretaceous of Madagascar. *J. Vertebr. Paleontol.* **18**, 562–568 (1998).
- Curry Rogers, K. A. in *The Sauropods: Evolution and Paleobiology* (eds Curry Rogers, K., Wilson, J. A.) 50–103 (University of California Press, 2005).
- Scheyer, T. M. & Sander, P. M. Histology of ankylosaur osteoderms: implications for systematics and function. *J. Vertebr. Paleontol.* **24**, 874–893 (2004).
- de Buffrénil, V., Farlow, J. & de Ricqlès, A. Growth and function of *Stegosaurus* plates: evidence from bone histology. *Paleobiology* **12**, 459–473 (1986).
- Main, R. P., de Ricqlès, A., Horner, J. R. & Padian, K. The evolution and function of thyreophoran dinosaur scutes: implications for plate function in stegosaurs. *Paleobiology* **31**, 291–314 (2005).
- Madsen, J. H. & Welles, S. P. *Ceratosaurs* (Dinosauria, Theropoda) a revised osteology. *Utah Geol. Surv. Misc. Pub.* **2**, 1–80 (2000).
- Rogers, R. R., Hartman, J. H. & Krause, D. W. Stratigraphic analysis of upper cretaceous rocks in the Mahajanga Basin, Northwestern Madagascar: implications for ancient and modern faunas. *J. Geol.* **108**, 275–301 (2000).
- Curry Rogers, K. The postcranial anatomy of *Rapetosaurus krausei* (Sauropoda: Titanosauria). *J. Vertebr. Paleontol.* **29**, 1046–1086 (2009).
- Ehrlich, H., Koutsoukos, P. G., Demadis, K. D. & Pokrovsky, O. S. Principles of demineralization: modern strategies for the isolation of organic frameworks Part II. Decalcification. *Micron* **40**, 169–193 (2009).
- Zylberberg, L. & Castanet, J. New data on the structure and growth of the osteoderms in the reptile *Anguis fragilis* L. (Anguillidae, Squamata). *J. Morphol.* **186**, 327–342 (1985).
- Francillon-Vieillot, H. et al. in *Skeletal Biomineralization: Patterns, Processes and Evolutionary Trends*, Vol 1 (ed. Carter, J. G.) 471–548 (Van Nostrand Reinhold, 1990).
- Vickaryous, M. K. & Hall, B. K. Osteoderm morphology and development in the nine-banded armadillo, *Dasypus novemcinctus* (Mammalia, Xenarthra, Cingulata). *J. Morphol.* **267**, 1273–1283 (2006).
- Levrat-Calviac, V. & Zylberberg, L. The structure of the osteoderms in the gekko *Tarentola mauritanica*. *Am. J. Anat.* **176**, 437–446 (1986).
- Depéret, C. Note sur les dinosaures sauroïdes et théropodes du Crétacé supérieur de Madagascar. *Bull. Soc. Géol. Fr.* **21**, 176–194 (1896).
- Rogers, R. R. Fine-grained debris flows and extraordinary vertebrate burials in the Late Cretaceous of Madagascar. *Geology* **33**, 297–300 (2005).
- Rogers, R. R., Krause, D. W., Curry Rogers, K., Rasoamimanana, A. H. & Rahantarisoa, L. Palaeoenvironment and Paleogeology of *Majungasaurus crenatissimus* (Theropoda: Abelisauridae) from the Late Cretaceous of Madagascar. *J. Vertebr. Paleontol. Memoir.* **8** 27 (suppl. to 2), 21–31 (2007).
- Upchurch, P., Barrett, P. M. & Dodson, P. in *The Dinosauria* 2nd edn (eds Weishampel, D. B., Dodson, P., Osmólska, H.) 259–322 (University of California Press, 2004).
- Seidel, M. R. The osteoderms of the American alligator and their functional significance. *Herpetologica* **35**, 375–380 (1979).
- Hutton, J. Age determination of living Nile crocodiles from the cortical stratification of bone. *Copeia* **1986**, 332–341 (1986).
- Hill, R. V. Comparative anatomy and histology of Xenarthran osteoderms. *J. Morphol.* **266**, 1441–1460 (2006).
- Drane, C. R. & Webb, G. J. W. Functional morphology of the dermal vascular system of the Australian lizard *Tiliqua scincoides*. *Herpetologica* **36**, 60–66 (1980).
- Rice, G. E. & Bradshaw, S. D. Changes in dermal reflectance and vascularity and their effects on thermoregulation in *Amphibolurus nuchalis* (Reptilia: Agamidae). *J. Comp. Physiol.* **135**, 139–146 (1980).

27. Rossman, T. Studien an känozoischen Krokodilen: 5. Biomechanische Untersuchung am postkranialen Skelett des paläogeonen Krokodils *Pristichampsus rollinatii* (Eusuchia: Pristichampsidae). *Neues Jahrb. Geol. Paläontol., Abhand.* **217**, 289–330 (2000).
28. Barboza, P. S., Parker, K. L. & Hume, I. D. *Integrative Wildlife Nutrition Volume II* (Springer, 2009).
29. Wysolmerski, J. J. The evolutionary origins of maternal calcium and b metabolism during lactation. *J. Mammary Gland. Biol.* **7**, 267–276 (2002).
30. Tucker, A. Validation of skeletochronology to determine age of freshwater crocodiles (*Crocodylus johnstoni*). *Mar. Freshwater Res.* **48**, 343–351 (1997).
31. Zippel, K. C., Lillywhite, H. B. & Mladinich, C. R. J. Anatomy of the crocodile spinal vein. *J. Morphol.* **258**, 327–335 (2003).
32. Sander, P. M. & Clauss, M. Sauropod Gigantism. *Science* **322**, 200–201 (2008).
33. Sander, P. M., Peitz, C., Jackson, F. D. & Chiappe, L. M. Upper Cretaceous titanosaur nesting sites and their implications for sauropod dinosaur reproductive biology. *Palaeontogr. Abt. A* **284**, 69–107 (2008).
34. Curtain, A. J., Zug, G. R. & Spotila, J. R. Longevity and growth strategies of the desert tortoise (*Gopherus agassizii*) in two American deserts. *J. Arid Environ.* **73**, 463–471 (2009).
35. Berry, K. H., Spangenberg, E. K., Homer, B. L. & Jacobson, E. R. Deaths of desert tortoises following periods of drought and research manipulation. *Chel. Cons. Biol.* **4**, 436–448 (2002).
36. Therrien, F., Zelenitsky, D. K. & Weishampel, D. B. Palaeoenvironmental reconstruction of the Late Cretaceous Sânpetru Formation (Haşeg Basin, Romania) using paleosols and implications for the ‘disappearance’ of dinosaurs. *Palaeogeogr. Palaeoclimatol. Palaeoecol.* **272**, 37–52 (2009).
37. Mohabey, D. M., Udhoji, S. G. & Verma, K. K. Palaeontological and sedimentological observations on non-marine Lameta Formation, Upper Cretaceous, India: their palaeoecological and palaeoenvironmental significance. *Palaeogeogr. Palaeoclimatol. Palaeoecol.* **105**, 83–94 (1993).
38. Ghosha, P., Bhattacharyab, S. K. & Janib, R. A. Palaeoclimate and palaeovegetation in central India during the Upper Cretaceous based on stable isotope composition of the palaeosol carbonates. *Palaeogeogr. Palaeoclimatol. Palaeoecol.* **114**, 285–296 (1995).
39. Sanchez, M. L., Gomez, M. J. & Heredia, S. Sedimentology and sedimentary paleoenvironments of Río Colorado Subgroup (Upper Cretaceous) Neuquén Group, in Neuquén City and surrounding areas. *Rev. Asoc. Geol. Argent.* **61**, 236–255 (2006).
40. Garcia, A. J. V., da Rosa, A. A. S. & Goldberg, K. Paleoenvironmental and paleoclimatic control on early diagenetic processes and fossil record in Cretaceous continental sandstones of Brazil. *J. South Am. Earth Sci.* **19**, 243–258 (2005).
41. González Riga, B. J. Bioestratigrafía y fosildiagénesis de un sitio paleontológico con saurópodos Titanosauridae del Cretácico Tardío de Mendoza, Argentina. *Ameghiniana* **40** (Suplemento Resúmenes), 58R (2003).

### Acknowledgements

We thank R. Hill for stimulating discussions in the early stages of this project, and acknowledge J. Diehm at North Star Imaging and J. Topich at Kinetic Vision for assistance with CT scanning and modelling of internal anatomy. B. Andres and K. Moffat assisted with histological coring of FMNH PR 2342. The work was supported by NSF grants (DEB-0822957 and EAR-0955716) to K.C.R. and by a grant in support of undergraduate research from OREL at Macalester College to A.C.

### Author contributions

K.C.R. and M.D. designed the study and, along with A.C., collected morphological data. K.C.R. and A.C. performed CT scans and histological analysis. M.V. was involved in data analysis, and R.R. provided the sedimentological and taphonomic context for the study. K.C.R. wrote the paper with contributions from M.D. All authors discussed results and commented on the manuscript.

### Additional information

**Supplementary Information** accompanies this paper at <http://www.nature.com/naturecommunications>

**Competing financial interests:** The authors declare no competing financial interests.

**Reprints and permission** information is available online at <http://npg.nature.com/reprintsandpermissions/>

**How to cite this article:** Curry Rogers, K. *et al.* Sauropod dinosaur osteoderms from the Late Cretaceous of Madagascar. *Nat. Commun.* **2**:564 doi: 10.1038/ncomms1578 (2011).